

Simulation of Grating Light Valves

E. P. Furlani

Eastman Kodak Company, Imaging Research and Advanced Development
Rochester, NY 14653-5305, USA, furlani@dtc.kodak.com

ABSTRACT

The Grating Light Valve (GLV) is a microelectromechanical reflection phase grating that operates on the electrostatic deflection of microbeams. In this paper we discuss a method for simulating GLVs. This method entails the solution of a nonlinear fourth-order beam equation with a forcing function, which is based on a parallel-plate capacitor model. We examine the accuracy of the force model using 2D finite element analysis (FEA). We show that this model renders force values that are within 90% of the FEA values. We also compute microbeam deflection profiles and switching voltages, and demonstrate that rigorous GLV simulations can be performed in a few minutes on a personal computer.

Keywords: Grating light valve, microbeam deflection, MEMS simulation, electrostatic analysis, finite element analysis.

INTRODUCTION

The Grating Light Valve (GLV), which was developed at Stanford by Bloom et al., is a microelectromechanical reflection phase grating consisting of flexible, metallic coated, silicon nitride beams suspended above a substrate (Fig. 1) [1]-[5]. The metallic coating on the beams serves both as an electrode, and as reflective surface for incident light. The substrate is also reflective and contains a separate electrode. When the beams are undeflected, the optical path-length difference between the beams and the substrate equals the wavelength of the incident light λ , and the grating reflects light as a flat mirror. However, when a sufficient voltage (switching voltage) is applied, the beams pull down to the substrate, thereby reducing the optical path-length difference to $\lambda/2$. Thus, light reflected from the beams is out of phase with that from the substrate and a diffraction pattern is formed (Fig. 1). Optical systems can intercept the diffracted light with output occurring only when the beams are activated. For display applications, a group of beams above a single substrate form an elemental pixel, and arrays of such pixels are fabricated to form an image [4].

In this paper, we discuss a method for predicting the deflection profile and switching voltage of the GLV

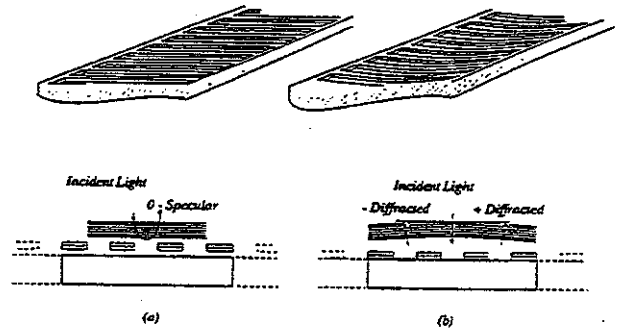


Fig. 1: GLV (a) undeflected, (b) deflected.

micronbeams. This method entails the solution of a nonlinear fourth-order beam equation, which is solved using a self-consistent, iterative, Green's function approach. The beam deflection force is based on a parallel plate capacitor model. We examine the accuracy of this model using 2D FEA. Specifically, we compute the electrostatic field and examine the effects of fringing. We also compute the electrostatic force and show that parallel plate model renders force values that are within 90% of the FEA values. Lastly, we compute beam deflection profiles and switching voltages for practical device parameters, and demonstrate that rigorous simulations can be performed in a few minutes on a personal computer.

THEORY

Consider the elemental microbeam shown in Fig. 2. The deflection of this structure is governed by the following equation

$$\frac{d^4 y}{dx^4} - \frac{\hat{T}}{EI} \frac{d^2 y}{dx^2} = \frac{F(y)}{EI} \quad (1)$$

where E and I are the Young's modulus and moment of inertia of the beam, respectively, $F(y)$ is the force

per unit length, and \hat{T} is the tensile force in the beam i.e., $\hat{T} = Tws$ where T , w , and s are the tensile stress, width, and thickness of the beam, respectively [6]. It is instructive to note that the GLV beam deflection is on the order of one hundredth of its length. Thus, the depth and slope of a plotted deflection profile tend to be exaggerated.

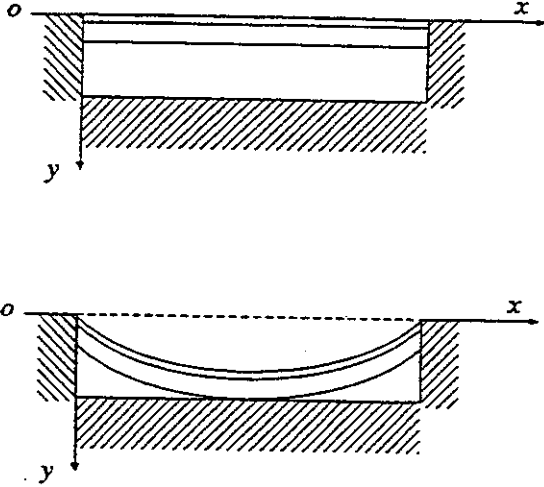


Fig. 2: Reference frame for mechanical analysis.

Force Model

The function $F(y)$ in (1) is given by the nonlinear parallel plate capacitor formula

$$F(y) = K_e \frac{V^2}{(\epsilon_0 s + \epsilon(h-y))^2}, \quad (2)$$

where $K_e = \frac{\epsilon^2 \epsilon_0 w}{2}$, V is the voltage, ϵ_0 and ϵ are the permittivities of free space and the beam, s is the thickness of the beam, and h is the distance from the bottom of an undeflected beam to the substrate. We investigate the accuracy of this model using FEA. Consider a single GLV microbeam of length L , width w , and thickness s . When the beam is undeflected the total distance between the "capacitor" electrodes is $h+s$. For a typical GLV, we have $\frac{L}{h+s} \approx 1000$, and $\frac{w}{h+s} \approx 4$. The parallel plate approximation is certainly valid for the length dimension. It remains to determine its validity for the cross-sectional dimension. To this end, we perform a 2D FEA with respect to this dimension.

We compute the electrostatic force between the beams and substrate using FEA, and then compare this result with the value obtained from (2) with $y=0$. Consider an infinite number of evenly spaced microbeams above a substrate (lengthwise into the page). We perform the FEA for three beams and impose boundary conditions that take into account the infinite array (Fig.

3)[3]. We set $V = 10$ volts, $L = 20 \mu\text{m}$, $w = 1.0 \mu\text{m}$, $s = 1250 \text{ \AA}$, $h = 1250 \text{ \AA}$ and $\epsilon = 6.45 \epsilon_0$. The thickness of the electrodes is 1000 \AA . The equipotential lines for this geometry are shown in Fig. 3b. The vertical field component beneath the beam, midway between the dielectric and the substrate, is shown in Fig. 4. Notice that the field obtains the parallel plate value of $6.926 \times 10^7 \text{ V/m}$ across approximately 70% of the width of the beam. Lastly, the FEA renders a force value of $F_{FEA} = 0.0236 \text{ N}$ between the electrodes. This compares to a value of $F(0) = 0.0212 \text{ N}$ as computed from (2) with $y=0$. Thus, the parallel plate formula (2) renders force values that are within 90% of rigorous values. Therefore (2) is well suited for GLV simulations.

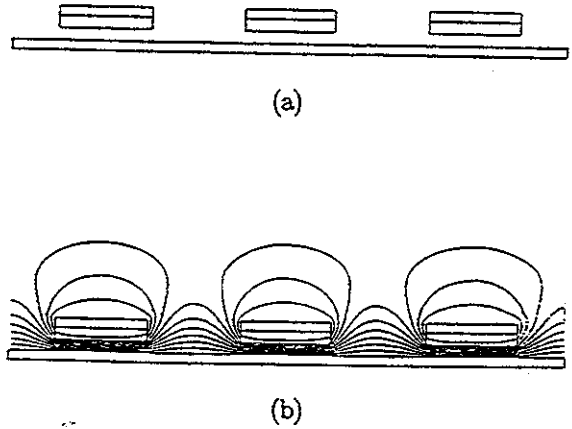


Fig. 3: (a) Beam array (b) Equipotential plot.

Deflection Analysis

We solve (1) using a self-consistent, iterative Green's function approach. The first step, is the determination of the Green's function $G(x, x')$ which satisfies

$$\frac{d^4 G(x, x')}{dx^4} - \frac{\hat{T}}{EI} \frac{d^2 G(x, x')}{dx^2} = \delta(x-x'). \quad (3)$$

The Green's function is derived from the homogeneous solution $y_h(x)$ that satisfies

$$\frac{d^4 y_h}{dx^4} - \frac{\hat{T}}{EI} \frac{d^2 y_h}{dx^2} = 0,$$

subject to the appropriate boundary conditions. It is well known that $y_h(x)$ is of the form $y_h(x) = a + bx + ce^{kx} + de^{-kx}$ where $k = \sqrt{\frac{\hat{T}}{EI}}$. Thus, $G(x, x')$ can be expressed as follows:

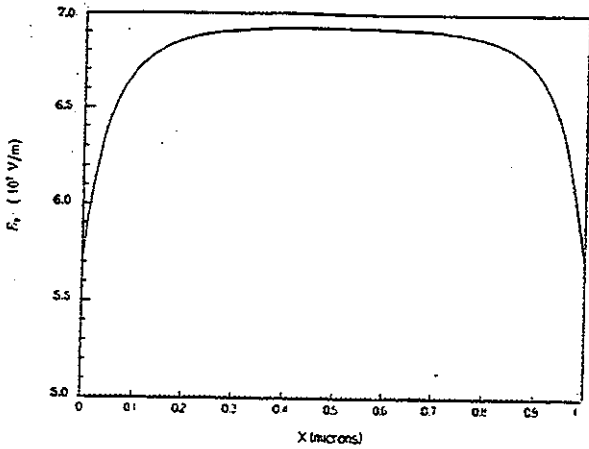


Fig. 4: E_y vs x between the beam and substrate.

$$G(x, x') = \begin{cases} f_1(x, x') & (x < x') \\ f_2(x, x') & (x > x') \end{cases} \quad (4)$$

where $f_i(x, x') = c_{i1}(x') + c_{i2}(x')x + c_{i3}(x')e^{kx} + c_{i4}(x')e^{-kx}$. The coefficients $c_{ij}(x')$, which are functions of x' , are determined from the boundary conditions that can be written in matrix form

$$B(x')C(x') = D, \quad (5)$$

where $B(x')$ is an 8×8 matrix that embodies the boundary conditions for $G(x, x')$ and

$$C^T = [c_{11}(x'), \dots, c_{14}(x'), c_{21}(x'), \dots, c_{24}(x')], \quad (6)$$

and

$$D^T = [0, 0, 0, 0, 0, 0, 0, 1], \quad (7)$$

(C^T denotes the transpose) [3]. For a given x' we solve (5) for $C(x')$,

$$C(x') = B^{-1}(x')D, \quad (8)$$

thereby determining the coefficients $c_{ij}(x')$, and hence $G(x, x')$.

Once $G(x, x')$ has been determined, we choose an initial beam profile $y^0(x)$, and perform a self-consistent iterative calculation of the form

$$y^{n+1}(x) = \int_0^L G(x, x')W(y^n(x')) dx^{prime}, \quad (9)$$

to determine a more accurate profile $y^1(x)$ [3][4]. This continues until the difference between successive profiles is within a specified tolerance ϵ , that is,

$$|y^{n+1}(x) - y^n(x)| < \epsilon \left| \frac{y^{n+1}(x) + y^n(x)}{2} \right| \quad (10)$$

for all $x \in [0, L]$. It is worth noting that when performing this analysis, care must be taken when inverting $B(x')$ because the values of k that one encounters render it illconditioned.

Hysteresis

The GLV beam deflection versus voltage profile exhibits a hysteresis like behavior (Fig. 5). This behavior can be understood by analyzing the beam deflection using a spring-capacitor model (Fig. 6). The spring represents the vertical component of the tensile force of the stretched beam, which is linear for small deflections, i.e.,

$$F_s(y) = K_s y, \quad (11)$$

where $K_s = \frac{4T}{L}$. The capacitor represents the electrostatic force between the beam and the substrate, i.e.,

$$F_e(y) = \tilde{K}_e \frac{V^2}{(\epsilon_0 s + \epsilon(h-y))^2}, \quad (12)$$

where $\tilde{K}_e = \frac{\epsilon^2 \epsilon_0 A}{2}$, and $A = wL$.

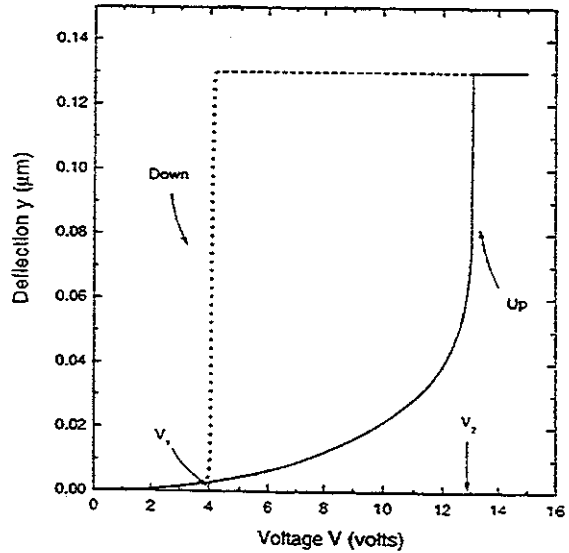


Fig. 5: Beam deflection $y(\frac{L}{2})$ vs V .

As illustrated in Fig. 5, the beam deflection, which is 0 when $V = 0$, gradually increases with voltage until the switching voltage V_2 is reached. When this happens, the beam snaps down to the substrate because the electrostatic force overwhelms the spring force, i.e., there is no intermediate deflection for which the spring and electrostatic force are in equilibrium. The beam stays fully deflected (against the substrate) as the voltage increases further.

Next, the voltage is reduced. As this happens, the electrostatic force decreases. However, it is sufficient

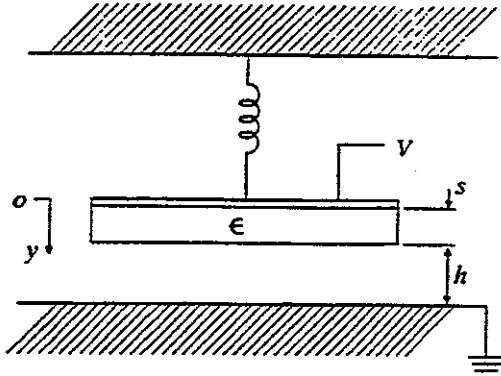


Fig. 6: Spring-capacitor model.

to hold the beam down even when the voltage drops below V_2 because the beam electrode is now closer to the substrate electrode than it was when the beam was initially pulled down [3]. Thus, the beam is stationary against the substrate until the voltage is reduced to V_1 , at which point the spring force overwhelms the electrostatic force and the beam snaps upward. Thus, as we cycle the voltage, the deflection versus voltage exhibits a hysteresis profile as shown.

Resonance

The resonant frequency of a microbeam can be estimated using the spring-capacitor model (Fig. 6). Specifically, we have $f = \frac{1}{2\pi} \sqrt{\frac{K_s}{m}}$ or, in terms of the material parameters

$$f_{res} = \frac{1}{L\pi} \sqrt{\frac{T}{\rho}}, \quad (13)$$

where T is the tensile stress and ρ is the density of the beam material ($\rho = 2.1 \text{ gm/cm}^3$ for silicon nitride)[1]. A plot of f_{res} versus L for several values of T is shown in Fig. 7.

Optical Analysis

Once the beam profile has been determined, the light intensity I_1 diffracted into the first-order mode can be computed. For normal incidence, I_1 is given by

$$I_1 = \frac{I_0}{2} \text{sinc}^2\left(\frac{\pi}{2}\right) (1 - \cos(\alpha)) \quad (14)$$

where

$$\alpha = \frac{2\pi(h + s - y(\frac{L}{2}))}{\lambda} \left(1 + \frac{1}{\sqrt{1 - \left(\frac{\lambda}{p}\right)^2}} \right),$$

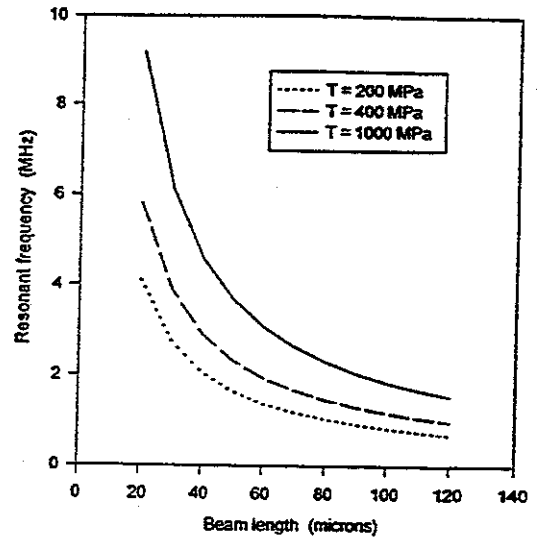


Fig. 7: Resonant frequency vs L .

I_0 is the incident intensity, $y(\frac{L}{2})$ is the deflection of the midpoint of the beam, λ is the wavelength of the incident light and p is the period of the grating [1]. This formula, which is derived using scalar diffraction theory, and is based on a grating comprising an infinite number of beams of infinite extent, renders reasonable predictions for practical devices [4].

SIMULATIONS

The beam deflection algorithm was implemented in FORTRAN and executed on a 120 Mhz Pentium computer. We applied it to a GLV with the following parameters: $T = 400 \text{ MPa}$, $L = 20 \text{ }\mu\text{m}$, $w = 1.0 \text{ }\mu\text{m}$, $s = 1350 \text{ \AA}$, $h = 1350 \text{ \AA}$ and $\epsilon = 6.45 \epsilon_0$. It took less than three minutes to compute the deflection versus voltage profile (approximately 10 sec per data point)(Fig. 5). The deflection values represent the positions of the midpoint of the beam $y(\frac{L}{2})$. Notice that the plot exhibits a hysteresis profile with switching voltages $V_1 = 3.6 \text{ v}$ and $V_2 = 12.5 \text{ v}$. The beam defelection profile y versus x was also computed in less than three minutes (Fig. 8).

We performed another series of calculations with the same parameters as above except for $s = 1300 \text{ \AA}$, and $h = 1300 \text{ \AA}$. The voltage V_2 was computed as a function of L for three different values of $T = 200, 400, 800 \text{ MPa}$ (Fig. 9). Notice that V_2 increases with tensile stress and decreases with beam length as expected. It took approximately 100 sec to compute each curve with 10 data points per curve.

ACKNOWLEDGEMENTS

The author would like to thank Enhua Lee for her help with some of the calculations in this manuscript.

REFERENCES

- [1] O. Solgaard, "Integrated Semiconductor Light Modulators for Fiber-Optic and Display Applications," Ph.D. Dissertation, Stanford University, 1992.
- [2] O. Solgaard, F.S.A. Sandejas, and D. M. Bloom, "A Deformable Grating Optical Modulator," *Opt. Lett.*, 17, (9), p.688, 1992.
- [3] R. B. Apte, "Grating Light Valves for High Resolution Displays," Ph.D. Dissertation, Stanford University, 1994.
- [4] F. S. A. Sandejas, "Silicon Microfabrication of Grating Light Valves," Ph.D. Dissertation, Stanford University, 1995.
- [5] E. P. Furlani, E. H. Lee, and H. Luo, "Analysis of Grating Light Valves with Partial Surface Electrodes," *J. Appl. Phys.* 83 (2), p. 629, 1998.
- [6] L. Meirovitch, "Analytical Methods in Vibrations," Macmillan Publishing, New York, 1967.

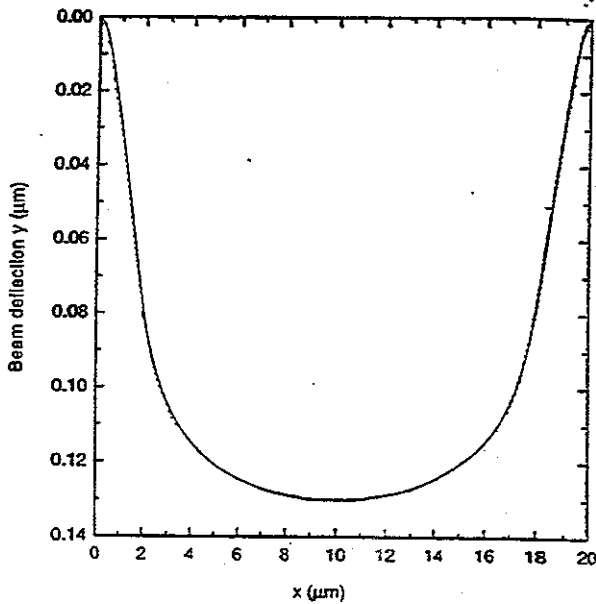


Fig. 8: Beam deflection profile y vs x .

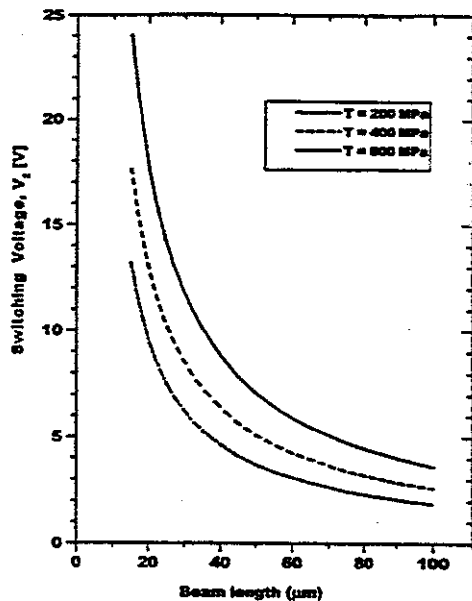


Fig. 9: Switching voltage V_2 vs L .

CONCLUSION

A method has been presented for simulating GLVs. This method can be readily implemented, and enables rapid parametric analysis of device performance. Our work demonstrates that rigorous GLV simulations can be performed in a few minutes on a personal computer.